

Comparison of Fura-2 Imaging and Electrophysiological Analysis of Murine Calcium Channel $\alpha 1$ Subunits Coexpressed with Novel $\beta 2$ Subunit Isoforms

ENRIQUE MASSA, KEVIN M. KELLY, DAVID I. YULE, ROBERT L. MACDONALD, and MICHAEL D. UHLER

Graduate Program in Neuroscience (E.M., M.D.U.), Mental Health Research Institute (M.D.U.), Department of Neurology (K.M.K., R.L.M.), Department of Physiology (D.I.Y., R.L.M.), and Department of Biological Chemistry (M.D.U.), University of Michigan, Ann Arbor, Michigan 48109-0720

Received August 12, 1994; Accepted January 23, 1995

SUMMARY

A polymerase chain reaction product was used to isolate mouse brain cDNA clones coding for isoforms of the β subunit of voltage-dependent Ca^{2+} channels. The two mouse brain $\beta 2$ subunit cDNA clones described, $\beta 2a$ and $\beta 2b$, differed by alternative splicing within the coding region but possessed a unique amino terminus not yet reported in other $\beta 2$ subunit cDNAs. Northern blot and RNase protection analyses demonstrated that both mRNA isoforms could be detected in highest abundance in heart and brain and at lower levels in lung, kidney, and testis. In a novel assay for $\beta 2$ subunit function, COS-1 cells were transfected with $\alpha 1$ and $\beta 2$ subunit expression vectors and assayed for increases in intracellular Ca^{2+} concentration by using fura-2 imaging. Co-transfection of COS-1 cells with the mouse brain class C-1 $\alpha 1$ subunit expression vector and either of the $\beta 2$ subunit expression vectors resulted in increases in intracellular Ca^{2+} concentration after stimulation with elevated K^+ and the dihydropyridine agonist

Bay K 8644. Transfection of either $\alpha 1$ or $\beta 2$ subunit expression vectors alone did not result in an elevation of intracellular Ca^{2+} concentration. Electrophysiological recording of human embryonic kidney 293 cells transfected with the expression vector for the $\alpha 1$ subunit alone or with either $\beta 2$ subunit demonstrated expression of voltage-dependent Ca^{2+} channels that were dihydropyridine sensitive. Currents formed by expression of only the $\alpha 1$ subunit were small and slowly inactivated. In contrast, the currents formed by coexpression of $\alpha 1$ subunits with either $\beta 2$ subunit were larger and inactivated more rapidly. Dihydropyridine binding studies demonstrated that coexpression of $\alpha 1$ subunits with $\beta 2$ subunits increased the density of functional receptors, compared with expression of $\alpha 1$ subunits alone. These experiments suggested that coexpression of the $\alpha 1$ and $\beta 2$ subunits produced functional dihydropyridine-sensitive Ca^{2+} channels and that both β subunit isoforms had modulatory effects on these channels.

The predominant pathway by which Ca^{2+} enters neurons, endocrine cells, and muscle cells is through voltage-dependent Ca^{2+} channels present in the plasma membrane (1-3). Influx of Ca^{2+} through voltage-dependent Ca^{2+} channels regulates a number of cellular functions, such as muscle contraction (4), neurotransmitter release (5), and gene expression (6). Based on their electrophysiological and pharmacological properties, these voltage-dependent Ca^{2+} channels have been classified into multiple types, including L, N, T, and P (2). The L-type channel is a high-threshold, slowly inactivating channel that is modulated by dihydropyridine agonists and antagonists. The N-type channel is a high-

threshold, rapidly inactivating channel that is blocked by the *Conus geographus* peptide toxin ω -conotoxin GVIA. The P-type channel is a high-threshold channel that is blocked by the peptide toxin ω -agatoxin IVa, isolated from the funnel web spider *Agelenopsis aperta*. In contrast to these channels, the T-type channel is a low-threshold channel that is preferentially blocked by Ni^{2+} .

Skeletal muscle contains the highest concentrations of voltage-sensitive Ca^{2+} channels that are of the L type (4). Purification of L-type channels from skeletal muscle led to the isolation of a protein complex composed of five subunits, $\alpha 1$, β , γ , $\alpha 2$, and δ (7). Molecular cloning of these different subunits has demonstrated molecular heterogeneity for $\alpha 1$ and β subunits. In contrast, $\alpha 2$, δ , and γ subunits do not exhibit such diverse molecular heterogeneity.

The $\alpha 1$ subunit is the largest of the five subunits and is an integral membrane protein. It also forms the ion-selective

This work was supported by the Lucille P. Markey Charitable Trust. E.M. was supported by Rackham Merit and R. W. Gerard Fellowships; D.I.Y. was supported by a Marion Merrell Dow fellowship and National Institutes of Health Grant DK41225.

ABBREVIATIONS: PCR, polymerase chain reaction; kb, kilobase(s); $[\text{Ca}^{2+}]_i$, intracellular calcium concentration; CMV, cytomegalovirus; PBS, phosphate-buffered saline; HEK, human embryonic kidney; bp, base pair(s); EGTA, ethylene glycol bis(β -aminoethyl ether)-*N,N,N',N'*-tetraacetic acid; HEPES, 4-(2-hydroxyethyl)-1-piperazineethanesulfonic acid.

pore through which Ca^{2+} flows into the cell (8). Molecular cloning of $\alpha 1$ subunits from rat brain suggests the existence of at least five different genes, each with several splice variants (9–13). The five classes of rat brain $\alpha 1$ subunits have been designated A, B, C, D, and E (9, 12). The class A $\alpha 1$ subunit gene may code for the P-type channel $\alpha 1$ subunit, but recent work demonstrated significant differences between recombinant currents and native P-type currents from neuronal cells (14). The class B $\alpha 1$ subunit gene has been shown to code for the N-type channel (13). The class C $\alpha 1$ subunit gene codes for cardiac L-type $\alpha 1$ subunits that are also expressed in smooth muscle and brain (15). The class D $\alpha 1$ subunit gene codes for a neuroendocrine L-type $\alpha 1$ subunit (16). The class E $\alpha 1$ subunit gene codes for an $\alpha 1$ subunit that forms a high-threshold current that is insensitive to dihydropyridines and ω -agatoxin IVA but is inhibited by Ni^{2+} (12, 17).

The $\alpha 2$, δ , and γ subunits are membrane-associated proteins (18–20). The $\alpha 2$ and δ subunits are derived by proteolysis of a precursor protein and are associated by disulfide bonds. To date, only one $\alpha 2$ isoform has been cloned. It was initially cloned from skeletal muscle and subsequently shown to be expressed in brain and heart as alternate splice variants (16). The γ subunit is a membrane-associated protein that was originally cloned from skeletal muscle (20). Attempts to clone this subunit from other tissues have been unsuccessful, suggesting that it is not a component of Ca^{2+} channels expressed in heart or brain (20). In addition, purification from brain demonstrated that neuronal L-type Ca^{2+} channels are composed of only $\alpha 1$, $\alpha 2\delta$, and β subunits (21).

In contrast to the $\alpha 1$, $\alpha 2$, and γ subunits, the β subunit is a cytoplasmic protein that is believed to associate tightly with the cytoplasmic domain of the $\alpha 1$ subunit (22). Molecular biological studies of β subunits suggest the existence of at least four different genes and several splice variants. The four classes of β subunits are designated as $\beta 1$ – $\beta 4$. $\beta 1$ is expressed in skeletal muscle and in brain as a splice variant (23, 24). $\beta 2$ is localized to cardiac and neuronal tissue (25). $\beta 3$ is found predominantly in brain and forms a component of N-type Ca^{2+} channels (26, 27). $\beta 4$ is expressed at high levels in cerebellum (28). Coexpression of cardiac and skeletal muscle L-type $\alpha 1$ subunits with various β subunit cDNAs demonstrated that the β subunit plays a major role in modulation and expression of functional Ca^{2+} channels. Expression of various β subunits with $\alpha 1$ subunits resulted in increased peak currents, altered rates of activation and inactivation, and increased density of functional channels (29–31).

The structural composition of neuronal Ca^{2+} channels is not well understood, due to their lower abundance and molecular heterogeneity. Recently we reported the cloning and expression of a mouse brain class C-I $\alpha 1$ subunit clone, which was able to form functional Ca^{2+} channels in cells that contain endogenous β subunit proteins (32). Here we report the cloning of two novel cDNA clones (mouse brain $\beta 2a$ and $\beta 2b$) that encode alternative splice variants of the $\beta 2$ gene. These cDNA clones were used to demonstrate that transient expression of either $\beta 2$ splice variant with the previously described murine calcium channel $\alpha 1$ subunit clone (mbC-I) can form functional dihydropyridine-sensitive Ca^{2+} channels. These channels were detected and characterized by fura-2 imaging, electrophysiological recordings, and dihydropyridine binding. In addition, this work examines differential effects of alternatively spliced $\beta 2$ subunits, which differ only in inter-

nal amino acid sequence. This work also characterizes the class C-I $\alpha 1$ subunit, which had not been previously examined using electrophysiological recordings.

Materials and Methods

Amplification of a rabbit skeletal muscle β subunit cDNA fragment from total RNA. Two oligonucleotide primers (GGTCTA-GACGGAGGAGAGGCTCCCTCCAT and CCGAATTCGTCAAA-CAAAGCTTTCTGCATCAT) were used to amplify a rabbit skeletal muscle β subunit cDNA fragment from rabbit skeletal muscle first-strand cDNA. The amplified product codes for a fragment containing sequence from nucleotide 136 to nucleotide 1052, based on the published rabbit skeletal muscle β subunit cDNA sequence (23). A PCR product of 916 bp was isolated on a 1% agarose gel. The isolated fragment was then digested with *EcoRI* and *XbaI* and ligated into *EcoRI/BglII*-digested pGEM-3Zf(+). After base denaturation, the resulting plasmids were sequenced with SP6 and T7 promoter primers, using a modified T7 DNA polymerase (Sequenase).

Mouse brain β subunit cDNA cloning and sequencing. Approximately 1.0×10^6 recombinant λ ZapII phage containing mouse brain cDNA fragments (Stratagene) were screened by hybridization as described previously (33). The 916-bp *EcoRI/XbaI* rabbit skeletal muscle β subunit cDNA fragment was labeled by random primer extension in the presence of [α - ^{32}P]dATP. The resulting radiolabeled DNA fragments were hybridized to phage DNA immobilized on Hybond-N membranes. Initially, six cDNA clones were isolated and sequenced with T3 and T7 promoter primers, using modified T7 DNA polymerase (Sequenase). One clone (mb $\beta 1$) encoded a splice variant of the mouse skeletal muscle β subunit that contained an open reading frame but lacked an initiator methionine. The 1.5-kb *EcoRI/XhoI* fragment from mb $\beta 1$ was isolated and labeled by random primer extension in the presence of [α - ^{32}P]dATP. The library was rescreened, resulting in the isolation of 54 additional clones. The cDNA inserts were sequenced with T3 and T7 promoter primers. Two clones, $\beta 2a$ and $\beta 2b$, were sequenced entirely. Sequence alignment of the amino acid sequences was performed using the Genetics Computer Group sequence analysis programs and reiterative alignment of the sequences using the GAP program. The sequences were submitted to the GenBank/EMBL Data Bank with accession number L20343.

Northern blot and RNase protection analyses. A 460-bp *EcoRI/SphI* cDNA fragment was isolated from $\beta 2a$, subcloned into *EcoRI/SphI*-digested pGEM-4, and sequenced. Plasmid was linearized with *EcoRI* and used as a template to generate antisense RNA probes for both β subunits. cRNA probes containing [α - ^{32}P]UTP (ICN Biochemicals) were generated using T7 RNA polymerase (BRL). RNase protection analysis using the 460-bp *EcoRI/SphI* fragment was performed according to previously described methods (34). Expression of $\beta 2a$ was detected by an asymmetric PCR-generated probe, encoding a 131-bp insert not found in $\beta 2b$. Two oligonucleotide primers (ATAGACATAGATGCTAC and CTTCTTAAAGAAGGGCA) were used to amplify a 131-bp fragment from the $\beta 2a$ cDNA template. The probe was amplified from the 131-bp fragment by asymmetric PCR using the second 3' oligonucleotide primer described above. The RNA blot (Clonetech) contained 2 μg of poly(A)⁺ RNA from the various tissues indicated and was the gift of Drs. Karen Martell and Jack Dixon (University of Michigan, Department of Biochemistry). After prehybridization for 4 hr, Northern blot hybridization with 1×10^6 cpm/ml cRNA or asymmetric PCR probe was performed at 60° overnight. The blot was washed at room temperature for 15 min in 2 \times SSPE (1 \times SSPE is 0.15 M NaCl, 5 mM NaH_2PO_4 , 1 mM EDTA) with 0.1% sodium pyrophosphate and 0.5% SDS, followed by washes at 37°, 50°, and 70°. Blots were subjected to autoradiography at -80°.

Construction of CMV. $\beta 2a$ and CMV. $\beta 2b$ expression vectors. A 2.1-kb or 1.97-kb *PstI/PstI* fragment was isolated from $\beta 2a$ or $\beta 2b$,

respectively. Each fragment was then ligated into the *Pst*I site of pBSBgI, a gift of Dr. Timothy Angelotti (University of Michigan, Department of Pharmacology). The pBSBgI plasmid was derived from pBluescript SK(-) that was digested with *Eco*RI and *Xho*I, end filled, and ligated with *Bgl*II linkers. The resultant plasmids were sequenced, and those containing an insert were digested with *Bam*HI and *Bgl*II. The cDNA fragments were isolated and ligated into the *Bgl*II site of pCMV.Neo (35). The resulting plasmids with the mb β 2a or mb β 2b coding region in the sense orientation were restriction mapped, sequenced to confirm orientation, and denoted pCMV.mb β 2a and pCMV.mb β 2b, respectively.

Transfection of COS-1 cells and fura-2 imaging. Two 10-cm plates containing COS-1 cells at 30% confluency were transfected, by calcium phosphate precipitation, with 10 μ g/plate of pCMV.mb β 2a or pCMV.mb β 2b, 10 μ g of pCMV.MCI (32), and 5 μ g of pCMV. β GAL, as described previously (36). COS-1 cells were also transfected with either pCMV.Neo, pCMV.mb β 2a, pCMV.mb β 2b, or pCMV.MCI alone. Thirty-six hours after application of the DNA precipitate, the cells were treated with trypsin, resuspended in 5 ml of buffer A (142 mM NaCl, 5.6 mM KCl, 2.2 mM CaCl₂, 3.6 mM NaHCO₃, 1 mM MgCl₂, 5.6 mM D-glucose, 30 mM HEPES, pH 7.4), and centrifuged for 5 min. The cells were resuspended in 5 ml of buffer A and incubated with 2 μ M fura-2/acetoxymethyl ester at room temperature for 30 min. The cells were then centrifuged and resuspended in fresh buffer A. For measurement of [Ca²⁺]_i, fura-2-loaded cells were transferred to a closed chamber mounted on the stage of a Zeiss Axiovert inverted microscope and were continuously superfused at 1 ml/min with buffer A, at 37°. Solution changes were rapidly accomplished by means of a valve attached to an eight-chambered superfusion reservoir. Activation and blockade of calcium channels were elicited by superfusion with 55.6 mM KCl and 1 μ M Bay K 8644 and were inhibited by 100 μ M nifedipine. Measurement of [Ca²⁺]_i was performed using a digital imaging system (Attofluor, Rockville, MD). Excitation of cells at 334 and 380 (10-nm bandpass) was accomplished with a computer-selectable filter and shutter system. Resultant emission at 510 nm was monitored with an intensified charge-coupled device camera and subsequently digitized. Calibration of [Ca²⁺]_i signals was performed by applying the equation of Grynkiewicz *et al.* (37). The fluorescent emission of external Ca²⁺ standards containing 1 μ M fura-2 either in the absence (1 mM EGTA) or in the presence of Ca²⁺ (1 mM) was monitored, allowing the determination of R_{max} , R_{min} , and β . The calibration was then applied to user-defined areas of interest, where gray level values were computed to give a measurement of [Ca²⁺]_i, as described previously (38).

Transfection of HEK 293 cells and electrophysiological recording. Six-centimeter plates containing HEK 293 cells at 75% confluency were transfected, by calcium phosphate precipitation, with 10 μ g/plate of pCMV. β 2a or pCMV. β 2b, 10 μ g of pCMV.MCI, and 1 μ g of pCMV. β GAL, as described previously (39). Twenty-four hours later, the cells were treated with trypsin, resuspended in 2 ml of Dulbecco's modified Eagle's medium, and incubated with 75 μ l of 10 mg/ml DNase I for 5 min. The cells were centrifuged and plated onto Mecanex-gridded dishes at a density of 100,000 cells/dish. Forty-eight hours after transfection, a β -galactosidase staining protocol was used to identify transfected cells (39). Cells were maintained in medium at 37°, rinsed with Dulbecco's phosphate buffered saline (PBS) (with Ca²⁺ and Mg²⁺), and returned to 37°. During incubation of the cells, 1 mM fluorescein di- β -galactopyranoside (a fluorescent *lacZ* substrate) in 0.5 \times PBS was warmed to 37°. Cells were removed from incubation, the PBS was aspirated, fluorescein di- β -galactopyranoside solution was added to the cells, and the culture dish was warmed at 37° for 1 min. The dish was then placed on ice and cold PBS was added. After 5 min, cells were viewed by fluorescence microscopy, to localize cells expressing β -galactosidase. After scoring of fluorescein-positive cells, the culture dish was removed for electrophysiological recordings.

Whole-cell voltage-clamp recordings of Ca²⁺ currents were made by the whole-cell variation of the patch-clamp technique. Recordings

were made using glass micropipettes (Fisher microhematocrit capillary tubes; inner diameter, 1.1 mm) pulled in four stages on a Brown-Flaming micropipette puller (model P-80) to 3–8 M Ω . Micropipettes were filled with a solution of 140 mM CsCl, 30 mM CsOH, 10 mM HEPES, 10 mM EGTA, 5 mM ATP, and 0.1 mM GTP, pH 7.3 (290 mOsm). Cells were bathed in a solution of 13 mM BaCl₂, 67 mM choline chloride, 100 mM tetraethylammonium chloride, 5.3 mM KCl, 1 mM MgCl₂, and 10 mM HEPES, pH 7.40 (330 mOsm). All experiments were conducted at room temperature.

Signals were led to an Axopatch 1-B patch-clamp amplifier (Axon Instruments, Burlingame, CA), which corrected pipette and whole-cell capacitance and series resistance by compensation circuitry. Typical input resistances were 500 M Ω to 1 G Ω . Series resistance was estimated by cancellation of the capacitance charging current transient after patch rupture. Series resistance compensation was 80–100% in most cases. After patch rupture, the cell was hyperpolarized to a holding potential of -80 mV. Voltage step commands were generated, digitized at 5.6 kHz, stored, and analyzed by a microcomputer (IBM AT) using the program pClamp 5.5.1 (Axon Instruments). Current traces were filtered with a Bessel filter at 10 kHz (-3 dB). Holding current was subtracted to base-line and leak currents were estimated using hyperpolarizing voltage commands of the same magnitude as the depolarizing commands used to evoke inward currents. The resulting current was assumed to be equal and opposite in magnitude to the leak current and was digitally subtracted from the recorded inward current to obtain the total Ba²⁺ current. Estimates of current magnitude and kinetic parameters were expressed as mean \pm standard error throughout.

Drugs were freshly prepared or taken from stock solutions on the day of the experiments, dissolved in external solution, and drawn up into blunt-tipped micropipettes (40–50 μ m) that were positioned about 50 μ m from the cell. Drugs were usually applied by passive diffusion before and during voltage step commands. Currents were evoked during delivery of the drug to attain a constant drug concentration at the cell. Micropipettes containing different drugs were substituted sequentially, with control and recovery trials, and were removed from the bath solution when not in use. Application of diluent alone had no effect on evoked currents.

(+)-[³H]PN200-110 binding to transfected HEK 293 cells. Ten-centimeter plates containing HEK 293 cells at 75% confluency were transfected, by calcium phosphate precipitation, with 10 μ g/plate of pCMV. β 2a or pCMV. β 2b, 10 μ g of pCMV.MCI, and 2 μ g of pCMV. β GAL, as described previously (39). Binding was determined as described previously (40), with the following modifications. Transiently transfected HEK 293 cells were harvested in 50 mM Tris-HCl, pH 7.4, homogenized in a homogenizer using a Teflon pestle, and centrifuged at 20,000 \times *g* for 20 min. Supernatants were assayed for β -galactosidase activity as described previously, to normalize transfection efficiency (35). Membrane pellets were resuspended in 50 mM Tris-HCl. Binding was assayed by incubation of 1 mg of membrane protein with 1 nM (+)-[³H]PN200-110. Nonspecific binding and total binding were determined by the addition of 1 μ M nifedipine or buffer, respectively. Binding reactions were incubated for 2 hr at 25° and were terminated by filtration through Whatman GF/C glass fiber filters, under vacuum, and washing with cold binding buffer. Bound radioligand was measured by liquid scintillation counting.

Results

Isolation of mouse brain cDNA clones for calcium channel $\beta 2$ subunits. A 916-bp cDNA fragment of the rabbit skeletal muscle β subunit was used to screen a mouse brain λ ZapII cDNA library. Evidence suggested that the skeletal muscle β subunit was expressed in brain; thus, a skeletal muscle β subunit was presumed to have a high probability of hybridizing to neuronal isoforms (24). The mouse brain $\beta 1$ cDNA, which was isolated first, encoded an incomplete splice

variant of the skeletal muscle $\beta 1$ subunit. A 1.5-kb *EcoRI/XbaI* fragment of $\beta 1$ was used to rescreen the library under low stringency conditions. Fifty-four additional cDNA clones were isolated by rescreening the library. Upon sequencing, two cDNA clones (mouse brain $\beta 2a$ and $\beta 2b$) were shown to encode splice variants homologous to the $\beta 2$ subunit described previously (25). The individual cDNA sequences were aligned to generate the composite cDNA and predicted amino acid sequences shown in Fig. 1. Both $\beta 2a$ and $\beta 2b$ have amino termini that differ significantly from the previously described rat $\beta 2$ sequence, up to amino acid 17. To date, an homologous amino-terminal sequence has not been described. The $\beta 2a$ cDNA contained 132 nucleotides, coding for amino acids 177–220, that were not present in mb $\beta 2b$. In contrast, $\beta 2b$ contained 18 nucleotides, which deleted amino acids 177–220 and replaced them with six amino acids. Putative cAMP-dependent protein kinase (Thr-171) and protein kinase C (Thr-30 and Ser-78, -149, -166, -197, -232, -242,

-352, -496, and -594) phosphorylation sites present in the β subunit isoforms are shown in Fig. 1.

Northern blot and RNase protection analysis of β subunit expression. To determine the relative expression of both $\beta 2a$ and $\beta 2b$ mRNA, Northern blot and RNase protection analyses were performed. Hybridization with an antisense $\beta 2a$ ^{32}P -labeled riboprobe demonstrated that $\beta 2$ -related mRNA was detected in heart, brain, lung, kidney, and testis. In these tissues three mRNAs, of approximately 6.0, 4.0, and 3.5 kb, were detected, as seen in Fig. 2A. As suggested for the rat $\beta 2$ mRNA (25), the three mRNA species may be due to alternative polyadenylation. The $\beta 2$ subunit mRNA was not detected in spleen, liver, or skeletal muscle. Hybridization with an antisense asymmetric PCR probe encoding a 132-bp insert found only in $\beta 2a$ detected mRNA in heart, brain, and lung, as seen in Fig. 2B. However, as shown in Fig. 2C, RNase protection analysis with antisense $\beta 2a$ detected expression of both isoforms in heart, brain, lung,

```

CTCCGTGGATCTGTGCCCTGGGTGCAGCTGCGGAAGATAAAGGCGCTACCCGGCTCATGAAGGCCACCTGGATCAGGCTTCTGAAAAGAGCCAAGGGAGGAAGGCTGAAGAGTTCGGACA 120
      M K A T W I R L L K R A K G G R L K S S D I 22
TCTGTGTTTCGGCAGACTCCTACACAGCCGCCATCCGATTTCAGATGTGTCTTTGGAAGAGGACCCGGAGGACGTACGTAGAGAAGCTGAGCGGCAGGCACAGGCACAGTTGGAAAAAG 240
  C G S A D S Y T S R P S D S D V S L E E D R E A V R R E A E R Q A Q A Q L E K A 62
CAAAGACAAAACCTGTTCAGTTTCAGTTCGGACCAATGTCAGATACAGCGCACGCCAGGAGGATGACGTTCCGGTGCCTGGCATGGCCATCTCCTTCGAGGCCAAAGATTTTCTGCATG 360
  K T K P V A F A V R T N V R Y S A R Q E D D V P V P G M A I S F E A K D F L H V 102
TTAAGAAAAATTTAATAATGACTGGTGGATAGGACGGCTGGTTAAAGAAGGCTGTGAAATCGGATTTATTCCAAGCCAGTCAAAGTACAGCAATGAGGCTCAGCAGCAACAGAGAG 480
  K E K F N N D W W I G R L V K E G C E I G F I P S P V K L E N M R L Q H E Q R A 142
CCAAGCAAGGAAAATCTATTCCAGTAAATCAGGAGGAAATCATCATCCAGTTTGGGTGACATAGTCCAGTTCAGAAAATCGACACCCGCTCATCTGCTATAGACATAGATGCTA 600
  K Q G K F Y S S K S G G N S S S S L G D I V P S S R K S T P P S S A I D I D A T 182
      [.....
      [.....
CTGCGTTAGATGCAGAAGAGAATGATATCCAGCAAACCACCGCTCCCTTAAGCCAGTGAACAGTGTAAACATCACCCCACTCCAAAGAGAAAAGAAATGCCCTTTTAAAGAAGACAG 720
  G L D A E E N D I P A N H R S P K P S A N S V T S P H S K E K R M P F F K K T E 222
      [.....AAGCAGAAGCAGAAGTCG]
      [.....K Q K Q K S ]
AGCACACTCTCTTATGATGTGGTACCTTCCATGCGACCACTGGTGTGGTGGGCCGTCTCTGAAGGGGTATGAGGTCACAGATATGATGCAAAAAGCACTGTTTATTGTTTCTAAAAC 840
  H T P P Y D V V P S M R P V V L V G P S L K G Y E V T D M M Q K A L F D F L K H 262
ACAGATTTGAAGGGGGATATCCATCACAAGAGTCACTGCTGACATCTCCCTTGCCAAAACGCTCAGTATTAACAATCCAGTAAGCATGCAATCATAGAAAAGTCCAAACACAAGGTCCA 960
  R F E G R I S I T R V T A D I S L A K R S V L N N P S K H A I I E R S N T R S S 302
GCTTAGCGGAAGTTTCAGAGTGAATTTGAAAGGATTTTGAAGTTCGAAAGTCACTGCAATTTGGTGTAGTCTTTCAGCGGATATAAATCACCAGCTCAACTCAGTAAGACCTTTTGG 1080
  L A E V Q S E I E R I F E L A R T L Q L V V L D A D T I N H P A Q L S K T S L A 342
CCCTATCATAGTGTACGTAAGAAATTTCTTCTCCCAAGGTTTACAAAGGTTGATAAAATCTCGAGGAAATCTCAAGAAAACACCTCAATGTCCAGATGGTAGCAGCTGATAAACTGG 1200
  P I I V Y V K I S S P K V L Q R L I K S R G K S Q A K H L N V Q M V A A D K L A 382
CCCAATGCTCTCCGAGGAATCATTGTATGTATCTTGGATGAGAACAGCTGGAGGACGCTTGTGAGCATCTTGCAGCATCTTGGAGGATACTGGAAGGCCACCCACCTCCAGCG 1320
  Q C P P Q E S F D V I L D E N Q L E D A C E H L A D Y L E A Y W K A T H P P S G 422
GTAACCTCCCAACCTCTGCTTAGCCGGACTTTAGCCCTCCTCAACTTTACCTCTGAGCCCCACCTCGCCTCTAATTCACAGGGTCTCAAGGTGATCAAAGGCTGATCGCTCTGCTC 1440
  N L P N P L L S R T L A S S T L P L S P T L A S N S Q G S Q G D Q R P D R S A P 462
CCCGTCTGCTTCCCAAGCTGAAGAAGAACTTGCCTAGAACCCGTCAAAAATCCCAACCCGTTCTCTCAGCCACACACAAAACCCGACGGGACAGGTCGAGGCCTCTCTA 1560
  R S A S Q A E E E P C L E P V K K S Q H R S S S A T H Q N H R S G T G R G L S R 502
GGCAAGAGAGCTTTGACTCTGAAACCAAGAGAGCCGAGACTCTGCCTACGTGGAGCCAAGGAAGATTATTACATGAACATGTGAGCCGGTATGTCCACACCCGAGCATAACCACA 1680
  Q E T F D S E T Q E S R D S A Y V E P K E D Y S H E H V D R Y V P H R E H N H R 542
GAGAGAGACCCACAGCAGCAATGGCCACAGACAGAGGAGTCTCGCCACCGCTCTAGGACATGGGTCGAGACAGGACCACAATGAGTGCATCAAACAACGAAGCCGGCATAAATCTA 1800
  E E T H S S N G H R H R E S R H R S R D M G R D Q D H N E C I K Q R S R H K S K 582
AGGATCGCTACTGTGACAAGGAGGGGAAGTAATATCCAAGAGAAGGAATGAGGCTGGCGAGTGAACAGGGATGTATACATCCGCCAATGACCGTGGTGTCCCTACCCCAAGTCTT 1920
  D R Y C D K E G E V I S K R R N E A G E W N R D V Y I R Q 611

TGTTGATCATCTTAAAGCAAAATCTTTGGGGTTACATTGCAACCA 1966

```

Fig. 1. Consensus sequence of mouse brain $\beta 2$ subunit cDNA clones. The consensus nucleotide sequence derived from the two independent cDNA clones is shown, with the predicted amino acid sequence below the nucleotide sequence. The region where alternatively spliced forms of cDNA clones were detected is indicated by the second nucleotide and amino acid sequences (in brackets) (nucleotides 585–716). Potential phosphorylation sites for cAMP-dependent protein kinase (Thr-171) and protein kinase C (Thr-30 and Ser-78, -149, -166, -167, -197, -232, -242, -352, -496, and -594) are underlined.

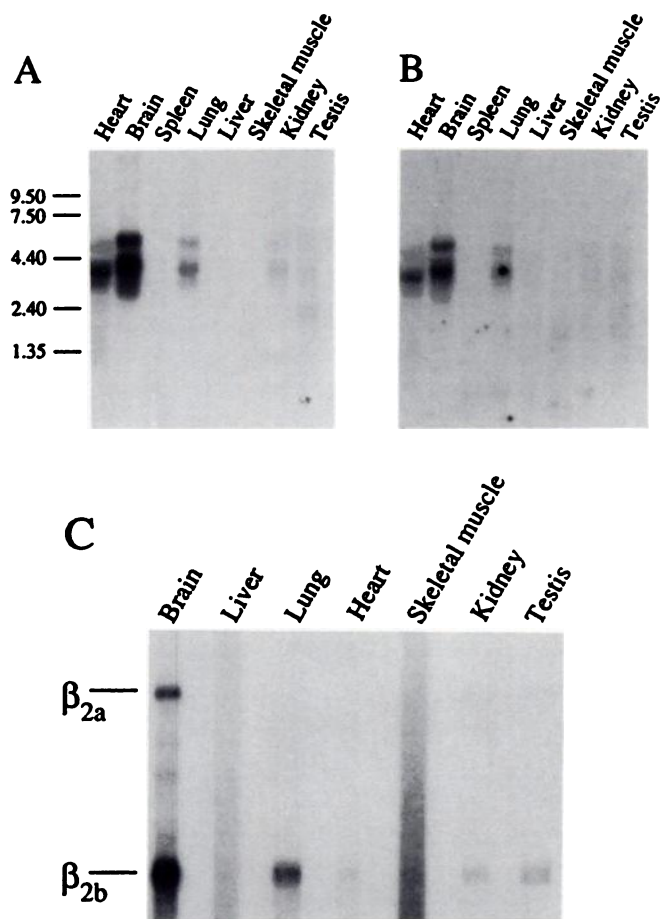


Fig. 2. Tissue distribution of $\beta 2$ subunit mRNA. RNA from various tissues was analyzed by Northern blot and RNase protection analyses as described in Materials and Methods. Numbers to the left, sizes of the RNA standards (in kb). A, Northern blot analysis of $\beta 2$ subunit mRNA expression in various tissues, determined by hybridization with an antisense riboprobe transcribed from a 460-bp *EcoRI/SphI* $\beta 2a$ fragment. B, Northern blot analysis of $\beta 2a$ subunit mRNA expression, determined by hybridization with an asymmetric PCR probe encoding a 126-bp insert found only in *mb\beta 2a*. C, RNase protection analysis of $\beta 2a$ and $\beta 2b$ subunit mRNA expression in tissues, determined by hybridization with the 460-bp *EcoRI/SphI* $\beta 2a$ fragment described for A.

kidney, and testis. This result was most likely due to the greater sensitivity of RNase protection assays and the low level of $\beta 2$ mRNA in kidney and testis.

Fura-2 imaging of transiently transfected COS-1 cells. To determine the functional expression of Ca^{2+} channels, COS-1 cells were transfected with both mouse brain class C-I $\alpha 1$ subunit and $\beta 2$ subunits, and fura-2 imaging was then performed to detect increases in $[\text{Ca}^{2+}]_i$ due to the influx of Ca^{2+} after depolarization-induced opening of Ca^{2+} channels. Increases in $[\text{Ca}^{2+}]_i$ in cells co-transfected with either $\beta 2$ subunit expression vector and the $\alpha 1$ subunit expression vector were measured after superfusion with the Ca^{2+} channel agonist Bay K 8644 and 55.6 mM KCl. Fura-2 imaging estimated an increase in $[\text{Ca}^{2+}]_i$ in individual cells from a large population, but only cells transfected with $\alpha 1$ and $\beta 2$ cDNAs responded to Bay K 8644 and KCl. Bay K 8644 and KCl did not stimulate an increase in $[\text{Ca}^{2+}]_i$ in mock-transfected cells or in cells transfected with either $\alpha 1$ or $\beta 2$ subunit cDNAs alone (Fig. 3, A–D). In contrast, $[\text{Ca}^{2+}]_i$ was increased in cells coexpressing $\beta 2a$ or $\beta 2b$ and $\alpha 1$ subunits by

as much as 250 nM (Fig. 3, E–H). Typically, 20–25% of imaged cells showed increased $[\text{Ca}^{2+}]_i$ upon perfusion with Bay K 8644 and KCl (Fig. 4B). The number of cells responsive to Bay K 8644 and KCl correlated well with the transfection efficiency, as determined by β -galactosidase staining (data not shown). Calcium channel activity was not observed during superfusion with Bay K 8644, KCl, and 100 μM nifedipine (Fig. 3, E and F).

Electrophysiological recordings of transiently transfected HEK 293 cells. Electrophysiological recordings were made from 172 transiently transfected, fluorescein-positive, HEK 293 cells with $\alpha 1$, $\alpha 1\beta 2a$, $\alpha 1\beta 2b$, or $\beta 2b$ subunit combinations. Interestingly, cells transfected with $\alpha 1$ subunits alone had greater viability than did $\alpha 1\beta 2$ subunit combinations under identical conditions of cell preparation and recording (data not shown). The percentages of fluorescein-positive cells from which currents could be evoked were as follows: $\alpha 1$, 51% (25 of 49 cells); $\alpha 1\beta 2a$, 40% (25 of 62 cells); $\alpha 1\beta 2b$, 36% (17 of 47 cells); $\beta 2b$, 0% (0 of 14 cells).

Currents evoked from cells transfected with $\alpha 1$ subunits alone were generally smaller than those from cells transfected with $\alpha 1\beta 2$ subunit combinations. Bay K 8644 (10 μM) was required to detect $\alpha 1$ currents in 40% (10 of 25) of cells but was required in only 7% (3 of 42) of cells with $\alpha 1\beta 2$ currents. The mean peak amplitude for cells expressing $\alpha 1$ subunit currents was 96.4 ± 27.2 pA ($n = 25$). The $\alpha 1$ subunit peak currents of >150 pA were enhanced by 67% ($n = 3$) upon application of Bay K 8644; $\alpha 1$ currents of <150 pA were undetected in the absence of Bay K 8644 (data not shown). Nifedipine (10 μM) blocked $\alpha 1$ currents by 80% within 2 min and by 100% with longer application times. There was no apparent voltage dependence of the current block by nifedipine (holding potentials of -80 to -40 mV and clamp potentials of -10 to 0 mV) (data not shown). Currents with peak amplitudes of <150 pA were difficult to assess and were not included in the analysis of kinetic parameters. The $\alpha 1$ subunits were activated to peak current rapidly, with an activation time of 20.8 ± 3.2 msec ($n = 4$). Representative current traces and a current-voltage relation for $\alpha 1$ currents are shown in Fig. 4A; they demonstrated that peak currents occurred at -10 mV and the reversal potential was 60 mV. Inactivation was slower for $\alpha 1$ subunit currents than for either $\alpha 1\beta 2$ subunit current (Fig. 5A) and the time to 50% inactivation (half-decay time) for $\alpha 1$ currents was 793.3 ± 13.3 msec ($n = 3$) (Fig. 5B).

Fig. 4, B and C, left, shows current traces for $\alpha 1\beta 2a$ and $\alpha 1\beta 2b$ subunit combinations, respectively. Peak amplitudes for $\alpha 1\beta 2$ subunit currents were 439.1 ± 109.3 pA ($n = 25$) ($\alpha 1\beta 2a$) and 397.8 ± 74.6 pA ($n = 16$) ($\alpha 1\beta 2b$). There was no significant difference between the mean peak current values for $\alpha 1\beta 2a$ and $\alpha 1\beta 2b$ currents (unpaired *t* test, $p = 0.76$). However, $\alpha 1\beta 2$ currents were significantly larger than $\alpha 1$ currents (unpaired *t* test, $p = 0.005$ for $\alpha 1\beta 2a$; $p = 0.001$ for $\alpha 1\beta 2b$). The $\alpha 1\beta 2$ control currents of >150 pA were enhanced by 62% ($n = 15$) upon addition of Bay K 8644 (10 μM). Bay K 8644 (10 μM) enhanced $\alpha 1\beta 2a$ and $\alpha 1\beta 2b$ currents in a manner similar to that described for $\alpha 1$ currents. Currents were activated fully by 23.2 ± 3.0 msec ($n = 6$) ($\alpha 1\beta 2a$) and 22.0 ± 2.9 msec ($n = 6$) ($\alpha 1\beta 2b$). There were no significant differences among the mean activation times to peak currents for $\alpha 1$, $\alpha 1\beta 2a$, and $\alpha 1\beta 2b$ currents (analysis of variance, $p = 0.87$). Fig. 4, B and C, right, shows the current-voltage rela-

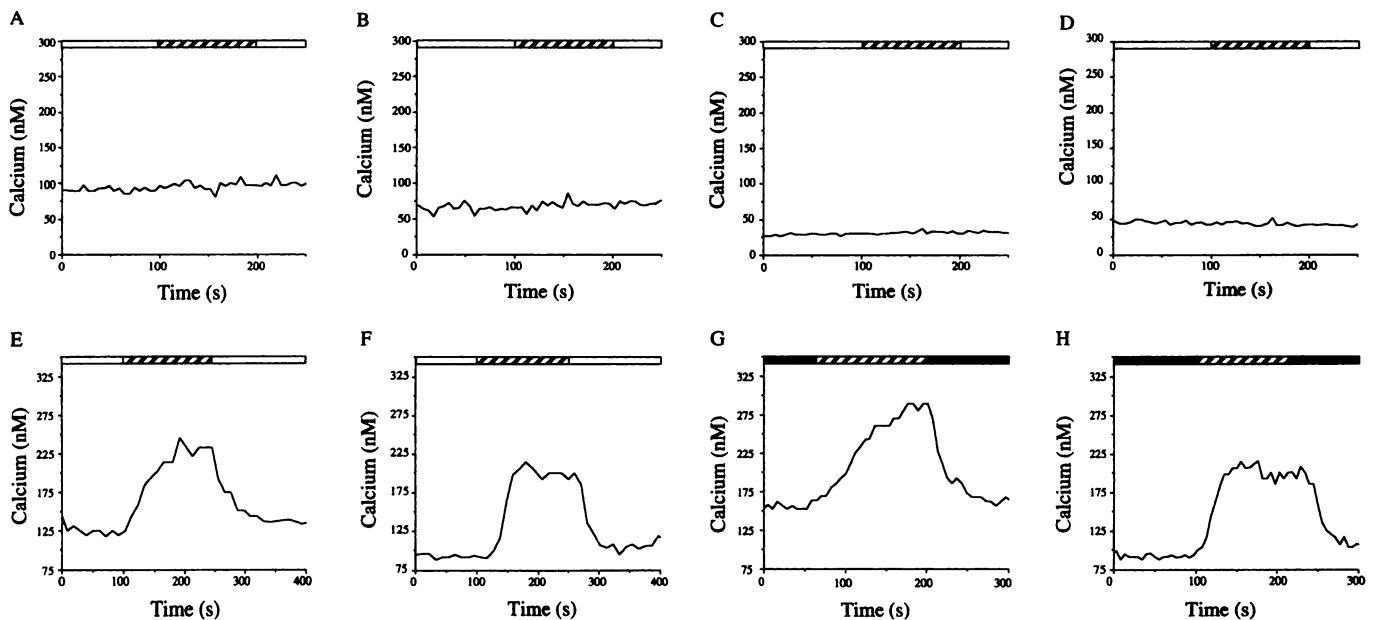


Fig. 3. Fura-2 imaging of transiently transfected COS-1 cells. Expression vectors were constructed as described in Materials and Methods. COS-1 cells were transfected, and 36 hr after transfection the cells were loaded with fura-2, superfused, and imaged as described in Materials and Methods. A, Transfection of COS-1 cells with pCMV.Neo. B, Transfection of COS-1 cells with pCMV.MC1. C, Transfection of COS-1 cells with pCMV. β 2a. D, Transfection of COS-1 cells with pCMV. β 2b. E and G, Co-transfection of COS-1 cells with pCMV.MC1 and pCMV. β 2a. F and H, Co-transfection of COS-1 cells with pCMV.MC1 and pCMV. β 2b. □, Perfusion with buffer A; ▨, perfusion with 1 μ M Bay K 8644 and 55.6 mM KCl; ■, perfusion with 1 μ M Bay K 8644, 55.6 mM KCl, and 100 μ M nifedipine. The expression experiments were repeated at least five times, and consistent results were obtained for each trial. The number of responsive cells correlated with the transfection efficiency, as determined by β -galactosidase staining.

tions for α 1 β 2a and α 1 β 2b subunits, respectively. Peak currents usually occurred at -10 mV (-20 mV for the α 1 β 2b combination shown). Reversal potentials calculated for different current-voltage relations were variable (44 mV for α 1 β 2a; 70 mV for α 1 β 2b) and not normalized to the Ba^{2+} equilibrium potential.

Fig. 5A shows representative α 1, α 1 β 2a, and α 1 β 2b currents normalized to peak current. Mean half-decay times were 440.2 ± 36.1 msec ($n = 5$) (α 1 β 2a) and 469 ± 31.9 msec ($n = 4$) (α 1 β 2b) (Fig. 5B). Mean half-decay times for α 1 currents (793.3 ± 13.3 msec, $n = 3$) were significantly longer (unpaired t test, $p = 0.0004$) than those for either α 1 β 2a or α 1 β 2b currents, which were not significantly different from each other (unpaired t test, $p = 0.58$). No cell transfected with the β 2b subunit alone ($n = 14$) demonstrated voltage-activated inward Ba^{2+} currents.

(+)-[3H]PN200-110 binding to transiently transfected HEK 293 cells. Fura-2 imaging and electrophysiological recordings demonstrated that the β 2 subunit increased the activity and current magnitude of α 1 subunit currents. To further examine the role of the β 2 subunit in modulation of the α 1 subunit, HEK 293 cells were transfected with the α 1 and β 2 subunit expression vectors and binding of a dihydropyridine ligand was determined. Binding of (+)-[3H]PN200-110 to membranes of transiently transfected HEK 293 cells demonstrated a 10-fold increase in dihydropyridine binding in cells coexpressing α 1 and β 2 subunits (Fig. 6). In contrast, cells transfected with α 1 subunits alone demonstrated a very low level of binding. Wild-type HEK 293 cells or cells transfected with either β 2 subunit alone did not demonstrate specific (+)-[3H]PN200-110 binding (data not shown).

Discussion

The two cloned mouse β subunit isoforms coded for alternate splice variants similar to the previously described rat and rabbit β 2 cDNAs, but these two murine isoforms contained a previously uncharacterized amino terminus (25, 41). Both isoforms were primarily expressed in heart and brain, but lower levels were detected in lung, kidney, and testis. Although similar splice variants internal to the coding region have been described for the β 2 subunit, the amino terminus found in both β 2a and β 2b (amino acids 1-17) has not been reported previously. The β 2a and β 2b subunits coded for cytoplasmic proteins that contain 611 and 572 amino acids, respectively, with predicted molecular weights of 68,930 for β 2a and 64,670 for β 2b. Both β 2 isoforms contained a high α -helical content, as reported for other previously cloned β subunit isoforms (23).

Voltage-dependent Ca^{2+} channels, especially in skeletal and cardiac muscle, are modulated by phosphorylation mediated by protein kinases (42). Phosphorylation of both skeletal muscle α 1 and β 1 subunits has been demonstrated (43). One consensus sequence for cAMP-dependent protein kinase (Arg-Lys-Ser-Thr-171) was present in both β 2a and β 2b, as shown in Fig. 1. This phosphorylation site was conserved in the rat, rabbit, and human skeletal muscle β 1 and cardiac/brain β 2 subunits (25, 44). Both β 2 subunits also contained several potential protein kinase C phosphorylation sites (Ser/Thr-X-Lys/Arg), as shown in Fig. 1. Previous work demonstrated that the β 1 subunit was phosphorylated by cAMP- and cGMP-dependent protein kinases and protein kinase C (43, 45). Although not fully demonstrated in any study to

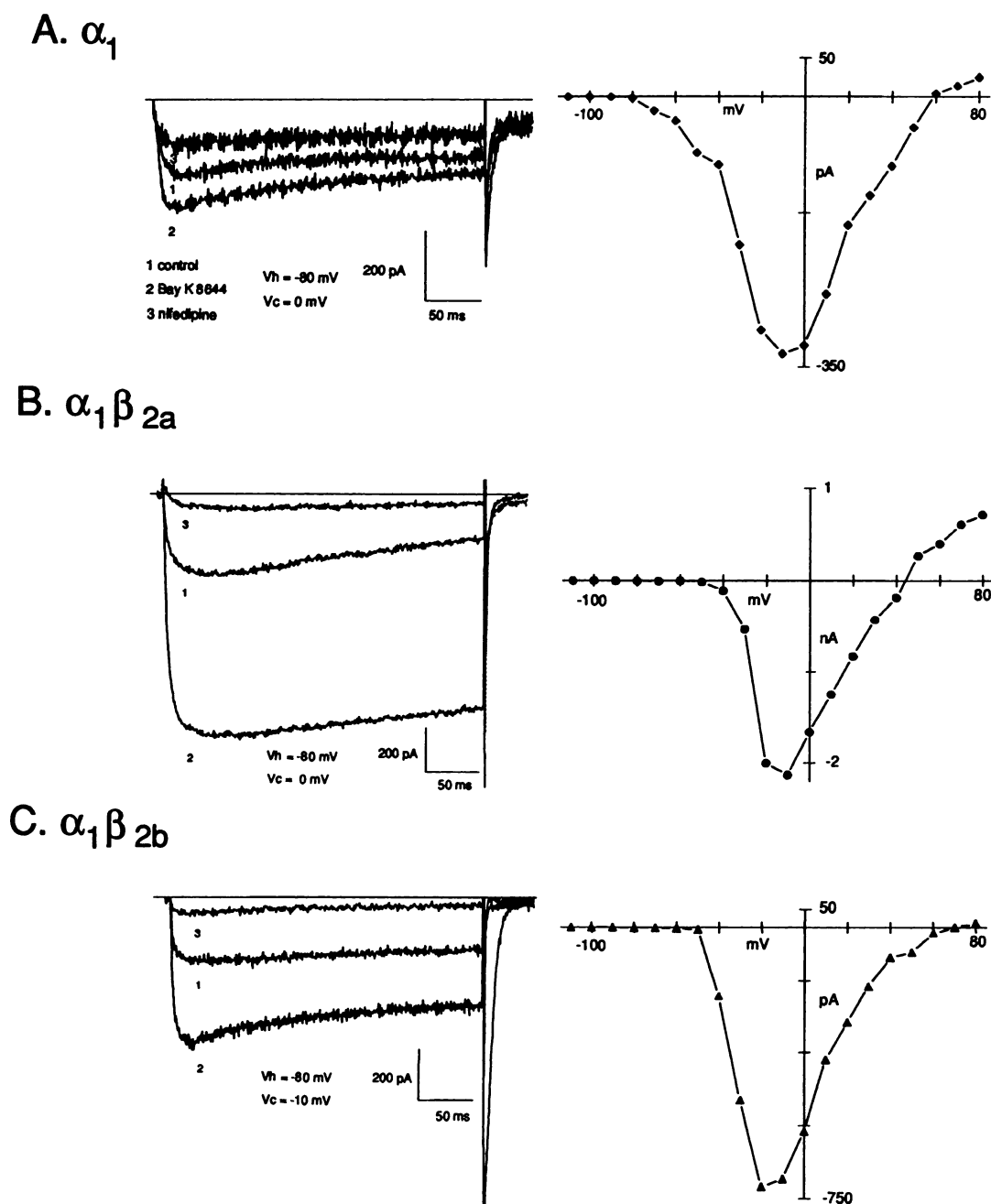


Fig. 4. Current traces and current-voltage relations for α_1 , $\alpha_1\beta_{2a}$, and $\alpha_1\beta_{2b}$ subunits expressed in HEK 293 cells. *Left*, Ba^{2+} current traces for α_1 (A), $\alpha_1\beta_{2a}$ (B), and $\alpha_1\beta_{2b}$ (C) subunit combinations, for control (1) and after application of Bay K 8644 (2) and nifedipine (3). Currents were evoked from a holding potential of -80 mV to clamp potentials of -10 or 0 mV as indicated. *Right*, current-voltage relations for α_1 (A), $\alpha_1\beta_{2a}$ (B), and $\alpha_1\beta_{2b}$ (C) subunits. Peak currents occurred in the range of -20 to -10 mV.

date, phosphorylation-dependent modulation of Ca^{2+} channels may involve phosphorylation of the β subunit.

To demonstrate that the $\beta 2$ cDNAs coded for functional β subunits, expression vectors coding for the full length $\beta 2a$ and $\beta 2b$ were constructed, using the human CMV promoter to direct their expression. The β subunit expression vectors were co-transfected with pCMV.MC1, the previously described mouse α_1 expression vector (32). Because transient transfection resulted in a high incidence of coexpression of two different plasmids (35, 46), those cells that expressed both α_1 and $\beta 2$ subunits were predicted to form functional Ca^{2+} channels. Because Ca^{2+} entry into cells via Ca^{2+} chan-

nels results in increased $[\text{Ca}^{2+}]_i$, we used fura-2 imaging to demonstrate functional expression of the α_1 and $\beta 2$ subunits. Although fura-2 imaging has been used to detect functional Ca^{2+} channels in neurons, fura-2 imaging has not been used to detect functional expression of recombinant voltage-dependent Ca^{2+} channels. Fura-2 imaging of recombinant Ca^{2+} channels is advantageous because large numbers of transfected cells can be assayed in a relatively short time and this technique measures the actual change in $[\text{Ca}^{2+}]_i$, which mediates many cellular responses to calcium.

Transfection of cells with α_1 and $\beta 2$ subunits formed functional Ca^{2+} channels that were activated by Bay K 8644 and

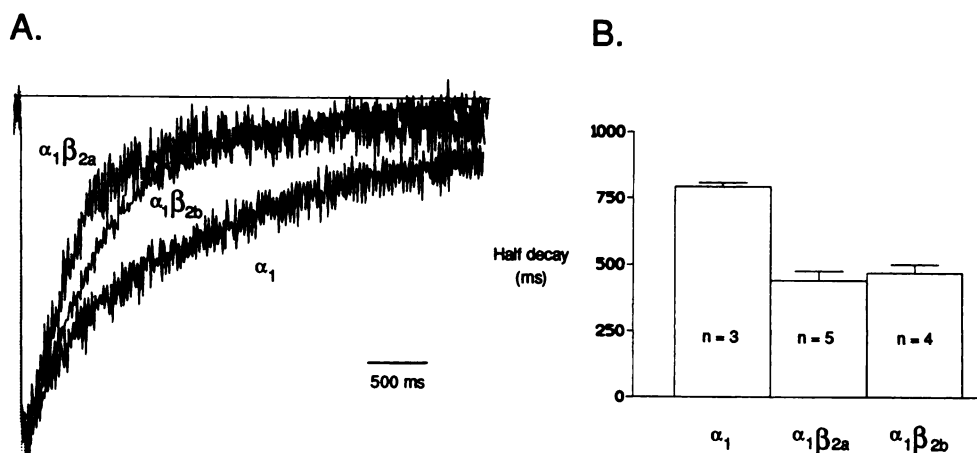


Fig. 5. Inactivation of currents evoked from α_1 , $\alpha_1\beta_{2a}$, and $\alpha_1\beta_{2b}$ subunits expressed in HEK 293 cells. **A**, Representative Ba^{2+} current traces from α_1 , $\alpha_1\beta_{2a}$, and $\alpha_1\beta_{2b}$ subunits normalized to peak current. Currents of similar magnitude for the different subunits were selected for comparison. Current inactivation for $\alpha_1\beta_{2a}$ and $\alpha_1\beta_{2b}$ subunits was faster than that for α_1 subunits. **B**, Difference in the time to 50% current inactivation (half-decay time) for α_1 , $\alpha_1\beta_{2a}$, and $\alpha_1\beta_{2b}$ subunit combinations.

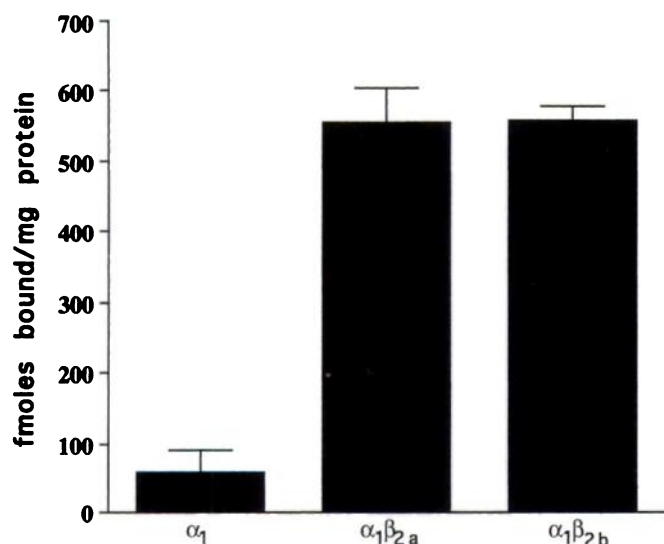


Fig. 6. Dihydropyridine binding to transiently transfected HEK 293 cell membranes. HEK 293 cells were transfected with the indicated subunit combinations and membranes were isolated after 48 hr. Membranes were incubated with (+)- ^3H PN200-110. Total and nonspecific binding was determined in the absence and presence of nifedipine, respectively. Binding was normalized to β -galactosidase expression and protein concentration. Transfection efficiency among the different transfections was consistent and showed no significant difference. Data represent the mean \pm standard deviation of a single transfection performed in triplicate. The binding was repeated twice for two separate transfections.

55.6 mM KCl. Nifedipine, a dihydropyridine antagonist, was able to inhibit the response to Bay K 8644 and 55.6 mM KCl. However, fura-2 imaging did not detect functional differences between the two β_2 subunit isoforms. Although previous electrophysiological analysis demonstrated that the class C cardiac α_1 subunit formed functional Ca^{2+} channels when expressed in oocytes, fura-2 imaging experiments reported here did not detect expression of functional Ca^{2+} channels in cells transfected with the α_1 subunit alone. Previously, Scatchard analysis of COS-1 cells transfected with the cardiac α_1 subunit alone demonstrated the presence of high affinity binding sites, but electrophysiological recordings were not performed (25). Cells expressing both the rat cardiac α_1 and

β_2 subunits expressed channels that had the same affinity for dihydropyridines but the number of binding sites was greatly increased, in comparison with cells expressing only the α_1 subunit (25). In addition, coexpression of α_1 and β subunits in oocytes produced larger Ca^{2+} channel currents, compared with those in oocytes expressing only the α_1 subunit (25). Thus, the inability of fura-2 imaging to detect functional channels in cells expressing the α_1 subunit alone may reflect a smaller population of functional channels that may also generate much smaller currents. The absence of detectable calcium channels in COS-1 cells expressing only the α_1 subunit, as well as the lack of differential effects of the two β_2 isoforms, prompted additional electrophysiological analysis of these calcium channel subunits.

To further examine the effect of the β_2 subunits on the α_1 subunit, HEK 293 cells were transfected with expression vectors and then Ca^{2+} channel activity was measured by whole-cell, patch-clamp, electrophysiological techniques, using Ba^{2+} as the charge carrier. This work is the first transient expression of neuronal, class C-I, dihydropyridine-sensitive, Ca^{2+} channels in mammalian cells. One consideration when Ca^{2+} channel subunits are expressed in oocytes is the presence of an endogenous, high-threshold, dihydropyridine- and ω -conotoxin GVIA-insensitive Ca^{2+} current (26). In contrast to *Xenopus* oocytes, mammalian cell lines such as HEK 293 do not express endogenous Ca^{2+} channel subunits or currents (data not shown).

Transfection of cells with the α_1 subunit alone or with either β_2 subunit expression vector led to the expression of high-threshold Ca^{2+} currents that were dihydropyridine sensitive (Fig. 4). Cells that were transfected with the β_{2b} subunit alone or mock transfected did not express Ba^{2+} currents (data not shown).

The α_1 subunit currents differed from the $\alpha_1\beta_2$ currents, and often α_1 subunit currents were undetectable in the absence of Bay K 8644. However, several cells expressed larger currents than could be detected in the absence of Bay K 8644. Activation and inactivation kinetics of the larger α_1 subunit currents were identical to those of the smaller currents, suggesting that the channels were identical. The $\alpha_1\beta_2$ subunit currents were of greater magnitude and were usually detected in the absence of Bay K 8644. Expression of either

$\beta 2$ subunit isoform was sufficient to potentiate the current magnitude in HEK 293 cells. The previously described rat $\beta 2$ subunit was demonstrated to increase the current magnitude 10-fold in oocytes expressing the rabbit cardiac $\alpha 1$ subunit (25). Activation kinetics of the mouse class C-I $\alpha 1$ subunit currents appeared to differ from those of the previously described cardiac, smooth muscle, and class C-II $\alpha 1$ subunit currents (25, 47, 48). The difference in activation kinetics for the class C-I $\alpha 1$ subunit currents may reflect the role of alternative splicing in the $\alpha 1$ subunit of voltage-dependent Ca^{2+} channels.

In comparison with $\alpha 1$ subunit currents, the activation time of $\alpha 1\beta 2$ subunit currents was identical but the inactivation time was shorter. Similar alterations of Ca^{2+} channel inactivation kinetics have been observed for other β subunit classes in oocytes (28). The altered inactivation kinetics of the $\alpha 1\beta 2$ subunit currents suggested that the β subunit plays several distinct roles in the modulation of the calcium channels. Alternative splicing of the $\beta 2$ subunit does not seem to differentially affect the function of the recombinant Ca^{2+} channel currents.

Fura-2 imaging and electrophysiological recordings demonstrated that the presence of $\beta 2$ subunits increased the current magnitude and inactivation rate of currents evoked from $\alpha 1$ subunits. Dihydropyridine binding demonstrated that the $\beta 2$ subunit increased the expression of dihydropyridine binding in transfected HEK 293 cells. The large increase in dihydropyridine binding in cells coexpressing the $\alpha 1$ and $\beta 2$ subunits may explain the absence of functional channels in fura-2-imaged COS-1 cells expressing only the $\alpha 1$ subunit, because the influx of calcium through $\alpha 1$ subunit channels may not increase $[\text{Ca}^{2+}]_i$ to levels detectable by fura-2 imaging. The increase in dihydropyridine binding also supported the observed increase in current magnitude when the $\beta 2$ subunit was coexpressed with the $\alpha 1$ subunit in HEK 293 cells. The mechanism of increased expression is unknown, although recent reports suggested that the β subunit modulates the dihydropyridine sensitivity of the $\alpha 1$ subunit and does not alter the relative expression of the $\alpha 1$ subunit (49, 50).

These experiments are significant for several reasons. First, expression of $\beta 2$ subunit isoforms with the previously uncharacterized class C-I $\alpha 1$ subunit demonstrated the effect of $\beta 2$ subunit coexpression on $\alpha 1$ subunit currents and suggests that $\beta 2$ subunit effects are relatively independent of the $\alpha 1$ subunit isoform that is coexpressed. In contrast to previous reports, the $\beta 2$ subunit did not alter the activation rate of $\alpha 1$ subunit currents. However, the $\beta 2$ subunit increased the inactivation rate of the $\alpha 1$ subunit currents. Coexpression of either the $\beta 2a$ or $\beta 2b$ subunit isoform increased the magnitude of the $\alpha 1$ subunit currents. Second, no distinct functional differences between the two $\beta 2$ subunits were detected. The alternative splicing of the β subunit may suggest a distinct role for these subunit isoforms in cellular localization or interaction with other accessory or modulatory proteins. Finally, the expression of these $\alpha 1$ and β subunit isoforms in mammalian cells is significant because previous expression of many neuronal Ca^{2+} channels has been achieved mainly by using *Xenopus* oocytes. In contrast to oocytes, the expression of Ca^{2+} channel subunits in mammalian cell lines such as COS-1 or HEK 293 permitted both fura-2 imaging and electrophysiological characterization of

recombinant Ca^{2+} channels in the absence of endogenous Ca^{2+} channel currents or subunits.

The $\alpha 1$ and $\beta 2$ subunit expression vectors should be useful for further characterization of the modulatory roles of the β subunit, especially when used in a rapid screening assay such as fura-2 imaging. Functional analysis of uncharacterized recombinant calcium channels would also be facilitated. Initial rapid screening would permit the optimization of transfection conditions and determination of pharmacological properties of the expressed currents without alterations of the intracellular environment. Detailed analysis could then be performed using electrophysiological recordings.

Furthermore, the comparison of electrophysiological properties of recombinant Ca^{2+} channels with experimentally determined $[\text{Ca}^{2+}]_i$ values may allow more detailed studies of the specific role of calcium entry via voltage-sensitive Ca^{2+} channels in the regulation of important cellular processes such as enzyme regulation and gene transcription. In addition to studies of the regulation of cellular processes, imaging and electrophysiological analysis should help to elucidate the regulation of recombinant Ca^{2+} channels by protein kinase-dependent phosphorylation.

Acknowledgments

The authors thank Linda Harper for assistance with cell culture, Timothy P. Angelotti for illuminating discussions, and Adele Barres for assistance in the preparation of the manuscript and figures.

References

1. Bean, B. P. Classes of calcium channels in vertebrate channels. *Annu. Rev. Physiol.* **51**:367–384 (1989).
2. Tsien, R. W., P. T. Ellinor, and W. A. Horne. Molecular diversity of voltage-dependent Ca^{2+} channels. *Trends Pharmacol. Sci.* **12**:349–354 (1991).
3. Miller, R. J. Voltage-sensitive Ca^{2+} channels. *J. Biol. Chem.* **267**:1403–1406 (1992).
4. Catterall, W. A. Excitation-contraction coupling in vertebrate skeletal muscle: a tale of two calcium channels. *Cell* **64**:871–874 (1991).
5. Miller, R. J. Receptor-mediated regulation of calcium channels and neurotransmitter release. *FASEB J.* **4**:3291–3299 (1990).
6. Murphy, T. H., P. F. Worley, and J. M. Baraban. L-type voltage-sensitive calcium channels mediate synaptic activation of immediate early genes. *Neuron* **7**:625–635 (1991).
7. Campbell, K. P., A. T. Leung, and A. H. Sharp. The biochemistry and molecular biology of the dihydropyridine-sensitive calcium channel. *Trends Neurosci.* **11**:425–430 (1988).
8. Catterall, W. A. Functional subunit structure of voltage-gated calcium channels. *Science (Washington D. C.)* **253**:1499–1500 (1991).
9. Snutch, T. P., J. P. Leonard, M. M. Gilbert, H. A. Lester, and N. Davidson. Rat brain expresses a heterogeneous family of calcium channels. *Proc. Natl. Acad. Sci. USA* **87**:3391–3395 (1990).
10. Snutch, T. P., W. J. Tomlinson, J. P. Leonard, and M. M. Gilbert. Distinct calcium channels are generated by alternative splicing and are differentially expressed in the mammalian CNS. *Neuron* **7**:45–57 (1991).
11. Starr, T. V., W. Prystay, and T. P. Snutch. Primary structure of a calcium channel that is highly expressed in the rat cerebellum. *Proc. Natl. Acad. Sci. USA* **88**:5621–5625 (1991).
12. Soong, T. W., A. Stea, C. D. Hodson, S. J. Dubel, S. R. Vincent, and T. P. Snutch. Structure and functional expression of a member of the low voltage-activated calcium channel family. *Science (Washington D. C.)* **260**:1133–1136 (1993).
13. Williams, M. E., P. F. Brust, D. H. Feldman, S. Patthi, S. Simerson, A. Maroufi, A. F. McCue, G. Velicelebi, S. B. Ellis, and M. M. Harpold. Structure and functional expression of an ω -conotoxin-sensitive human N-type calcium channel. *Science (Washington D. C.)* **257**:389–395 (1993).
14. Sather, W. A., T. Tanabe, J. F. Zhang, Y. Mori, M. E. Adams, and R. W. Tsien. Distinctive biophysical and pharmacological properties of class A (BI) calcium channel $\alpha 1$ subunits. *Neuron* **11**:291–303 (1993).
15. Mikami, A., K. Imoto, T. Tanabe, T. Niidome, Y. Mori, H. Takeshima, S. Narumiya, and S. Numa. Primary structure and functional expression of the cardiac dihydropyridine-sensitive calcium channel. *Nature (Lond.)* **340**:230–233 (1989).
16. Williams, M. E., D. H. Feldman, A. F. McCue, R. Brenner, G. Velicelebi, S. B. Ellis, and M. M. Harpold. Structure and functional expression of $\alpha 1$, $\alpha 2$,

- and β subunits of a novel human neuronal calcium channel subtype. *Neuron* 8:71–84 (1992).
17. Ellinor, P. T., J. F. Zhand, A. D. Randall, M. Zhou, T. L. Schwarz, R. W. Tsien, and W. A. Horne. Functional expression of a rapidly inactivating neuronal calcium channel. *Nature (Lond.)* 363:455–458 (1993).
 18. De Jongh, K. S., C. Warner, and W. A. Catterall. Subunits of purified calcium channels: $\alpha 2$ and δ are encoded by the same gene. *J. Biol. Chem.* 265:14738–14741 (1990).
 19. Jay, S. D., A. H. Sharp, S. D. Kahl, T. S. Vedvick, M. M. Harpold, and K. P. Campbell. Structural characterization of the dihydropyridine-sensitive calcium channel $\alpha 2$ -subunit and the associated δ peptides. *J. Biol. Chem.* 266:3287–3293 (1991).
 20. Jay, S. D., S. B. Ellis, A. F. McCue, M. E. Williams, T. S. Vedvick, M. M. Harpold, and K. P. Campbell. Primary structure of the γ subunit of the DHP-sensitive calcium channel from skeletal muscle. *Science (Washington D. C.)* 248:490–492 (1990).
 21. Ahljianian, M. K., R. E. Westenbroek, and W. A. Catterall. Subunit structure and localization of dihydropyridine-sensitive calcium channels in mammalian brain, spinal cord, and retina. *Neuron* 4:819–832 (1990).
 22. Leung, A. T., T. Imagawa, B. Block, C. Franzini-Armstrong, and K. P. Campbell. Biochemical and ultrastructural characterization of the 1,4-dihydropyridine receptor from rabbit skeletal muscle: evidence for a 52,000 Da subunit. *J. Biol. Chem.* 263:994–1001 (1988).
 23. Ruth, P., A. Rohrkasten, M. Biel, E. Bosse, S. Regulla, H. E. Meyer, V. Flockerzi, and F. Hofmann. Primary structure of the β subunit of the DHP-sensitive calcium channel from skeletal muscle. *Science (Washington D. C.)* 245:1115–1118 (1989).
 24. Pragnell, M., J. Sakamoto, S. D. Jay, and K. P. Campbell. Cloning and tissue-specific expression of the brain calcium channel β -subunit. *FEBS Lett.* 291:253–258 (1991).
 25. Perez-Reyes, E., A. Castellano, H. S. Kim, P. Bertrand, E. Bagstrom, A. E. Lacerda, X. Y. Wei, and L. Birnbaumer. Cloning and expression of a cardiac/brain β subunit of the L-type calcium channel. *J. Biol. Chem.* 267:1792–1797 (1992).
 26. Castellano, A., X. Wei, L. Birnbaumer, and E. Perez-Reyes. Cloning and expression of a third calcium channel β subunit. *J. Biol. Chem.* 268:3450–3455 (1993).
 27. Witcher, D. R., M. De Waard, J. Sakamoto, C. Franzini-Armstrong, M. Pragnell, S. D. Kahl, and K. P. Campbell. Subunit identification and reconstitution of the N-type Ca^{2+} channel complex purified from brain. *Science (Washington D. C.)* 261:486–489 (1993).
 28. Castellano, A., X. Wei, L. Birnbaumer, and E. Perez-Reyes. Cloning and expression of a neuronal calcium channel β subunit. *J. Biol. Chem.* 268:12359–12366 (1993).
 29. Singer, D., M. Biel, I. Lotan, V. Flockerzi, F. Hofmann, and N. Dascal. The roles of the subunits in the function of the calcium channel. *Science (Washington D. C.)* 253:1553–1557 (1991).
 30. Wei, X. Y., E. Perez-Reyes, A. E. Lacerda, G. Schuster, A. M. Brown, and L. Birnbaumer. Heterologous regulation of the cardiac Ca^{2+} channel $\alpha 1$ subunit by skeletal muscle β and γ subunits: implications for the structure of cardiac L-type Ca^{2+} channels. *J. Biol. Chem.* 266:21943–21947 (1991).
 31. Lacerda, A. E., H. S. Kims, P. Ruth, E. Perez-Reyes, V. Flockerzi, F. Hofmann, L. Birnbaumer, and A. M. Brown. Normalizations of current kinetics by interaction between the $\alpha 1$ and β subunits of the skeletal muscle dihydropyridine-sensitive Ca^{2+} channel. *Nature (Lond.)* 352:527–530 (1991).
 32. Ma, W. J., R. W. Holz, and M. D. Uhler. Expression of a cDNA for a neuronal calcium channel $\alpha 1$ subunit enhances secretion from adrenal chromaffin cells. *J. Biol. Chem.* 267:22728–22732 (1992).
 33. Olsen, S. R., and M. D. Uhler. Isolation and characterization of cDNA clones for an inhibitor protein of cAMP-dependent protein kinase. *J. Biol. Chem.* 266:11158–11162 (1991).
 34. Zinn, K., D. DiMaio, and T. Maniatis. Identification of two distinct regulatory regions adjacent to the human β -interferon gene. *Cell* 34:865–879 (1983).
 35. Huggenvik, J. I., M. W. Collard, R. E. Stofko, A. F. Seasholtz, and M. D. Uhler. Regulation of the human enkephalin promoter by two isoforms of the catalytic subunit of cyclic adenosine 3',5'-monophosphate-dependent protein kinase. *Mol. Endocrinol.* 5:921–930 (1991).
 36. Olsen, S. R., and M. D. Uhler. Inhibition of protein kinase-A by overexpression of the cloned human protein kinase inhibitor. *Mol. Endocrinol.* 5:1246–1256 (1991).
 37. Gryniewicz, G., M. Poenie, and R. Y. Tsien. A new generation of Ca^{2+} indicators with greatly improved fluorescence properties. *J. Biol. Chem.* 260:3440–3450 (1985).
 38. Brooker, G., T. Seki, D. Croll, and C. Wahlestedt. Calcium wave evoked by activation of endogenous or exogenously expressed receptors in *Xenopus* oocytes. *Proc. Natl. Acad. Sci. USA* 87:2813–2817 (1990).
 39. Angelotti, T. P., M. D. Uhler, and R. L. Macdonald. Assembly of GABA_A receptor subunits: analysis of transient single-cell expression utilizing a fluorescent substrate/marker gene technique. *J. Neurosci.* 13:1418–1428 (1993).
 40. Nikodijevic, B., D. Nikodijevic-Kedeva, M. Oshima, B. Paige, and G. Guroff. The long-term down-regulation of dihydropyridine receptors by Bay K 8644 in PC-12 cells. *J. Neurosci. Res.* 37:71–82 (1994).
 41. Hulin, R., D. Singer-Lahat, M. Freichel, M. Biel, N. Dascal, F. Hofmann, and V. Flockerzi. Calcium channel β subunit heterogeneity: functional expression of cloned cDNA from heart, aorta and brain. *EMBO J.* 11:885–890 (1992).
 42. Trautwein, W., and J. Hescheler. Regulation of cardiac L-type calcium current by phosphorylation and G proteins. *Annu. Rev. Physiol.* 52:257–274 (1990).
 43. De Jongh, K. S., D. K. Merrick, and W. A. Catterall. Subunits of purified calcium channels: a 212 kDa form of $\alpha 1$ and partial amino acid sequence of a phosphorylation site of an independent β subunit. *Proc. Natl. Acad. Sci. USA* 86:8285–8289 (1989).
 44. Collin, T., J. J. Wang, J. Nargeot, and A. Schwartz. Molecular cloning of three isoforms of the L-type voltage-dependent calcium channel β subunits from normal human heart. *Circ. Res.* 72:1337–1344 (1993).
 45. Mery, P. F., S. M. Lohmann, U. Walter, and R. Fischmeister. Ca^{2+} current is regulated by cyclic GMP-dependent protein kinase in mammalian cardiac myocytes. *Proc. Natl. Acad. Sci. USA* 88:1197–1201 (1991).
 46. Pritchett, D. B., H. Sontheimer, C. M. Gorman, H. Kettenmann, P. H. Seeburg, and P. R. Schofield. Transient expression shows ligand gating and allosteric potentiation of GABA_A receptor subunits. *Science (Washington D. C.)* 242:575–578 (1988).
 47. Welling, A., E. Bosse, A. Cavalie, R. Bottlender, A. Ludwig, W. Nastainczyk, V. Flockerzi, and F. Hofmann. Stable co-expression of calcium channel $\alpha 1$, β and $\alpha 2/\delta$ subunits in a somatic cell line. *J. Physiol. (Lond.)* 471:749–765 (1993).
 48. Tomlinson, W. J., A. Stea, E. Bourinet, P. Charnet, J. Nargeot, and T. P. Snutch. Functional properties of a neuronal class C L-type calcium channel. *Neuropharmacology* 32:117–126 (1993).
 49. Neely, A., X. Wei, R. Olcese, L. Birnbaumer, and E. Stefani. Potentiation by the β subunit of the ratio of the ionic current to the charge movement in the cardiac calcium channel. *Science (Washington D. C.)* 262:575–578 (1993).
 50. Nishimura, S., H. Takeshima, F. Hofmann, V. Flockerzi, and K. Imoto. Requirement of the calcium channel β subunit for functional conformation. *FEBS Lett.* 324:283–286 (1993).

Send reprint requests to: Michael D. Uhler, Neuroscience Laboratories Building, University of Michigan, 1103 East Huron, Ann Arbor, MI 48109–1687.
